THE STRUCTURE OF ZnTPP, ZnTPP-C_{60} THIN FILMS AND X-RAY EFFECT ON THEIR PHOTOLUMINESCENCE

N.M. Romanov[1,2], I.B. Zakharova[1], M.A. Elistratova[3], E. Lähderanta[2]

[1] Peter the Great St. Petersburg Polytechnic University, St. Petersburg, Russian Federation;

[2] Lappeenranta University of Technology, Lappeenranta, Finland;

[3] Ioffe Institute of RAS, St. Petersburg, Russian Federation

The paper presents the results of studies in properties of ZnTPP and nanocomposite ZnTPP-C_{60} films prepared under quasi-equilibrium conditions. The films' composition, structure and surface morphology have been investigated. Inequality in the optical absorption and photoluminescence (PL) spectra of ZnTPP solution and ZnTPP film was testimony to the formation of a regulated phase with the 745 nm-phosphorescence at room temperature. The X-ray effect on the PL spectra of ZnTPP and ZnTPP-C_{60} films was considered. The former was rather stable to the used X-ray doses. The dose dependences of electronic and electron-vibrational contributions to the PL emission intensity were different for the latter. A decrease in the emission intensity due to the electronic transition in the composite was caused by a probability increase in an excitation transfer from the carrier to the fullerene C_{60} and, correspondingly, by PL suppression.

Key words: metalloporphyrin; nanocomposite; fullerene; photoluminescence; X-radiation; scanning electron microscopy; X-ray diffractometry

Citation: N.M. Romanov, I.B. Zakharova, M.A. Elistratova, E. Lähderanta, The structure of ZnTPP, ZnTPP-C_{60} thin films and X-ray effect on their photoluminescence, St. Petersburg State Polytechnical University Journal. Physics and Mathematics. 11 (2) (2018) 19 – 30. DOI: 10.18721/JPM.11203

Introduction

Recent studies in organic nanoelectronics have paid much attention to nanocomposites with bulk heterojunctions [1, 2]. Vacuum deposition (thermal evaporation in vacuum) of thin films from initial mixtures is an industrial method of obtaining structures with bulk heterojunctions [3]. Different molecular components of porphyrins and phthalocyanins are successfully used as initial materials [4]; one example is tetraphenylporphyrin (H_2TPP), a derivative compound of porphin ($C_{20}H_{14}N_4$). The latter consists of four pyrrole rings with methine bridges. Pyrrole rings are five-membered aromatic nitrogen heterocycles.

Chelates (metal complexes of porphyrins, or MeTPP) are some of the most promising materials from the porphyrin group for applications in organic optoelectronics. A metal ion replacing two hydrogen atoms is located at the core of a tetrapyrrolic macrocycle. This macrocyclic structure has a high degree of π-conjugation, which regulates its main properties, for example, absorption of light in different spectral regions and fluorescence; the chelate has a strong donor effect [5].

Porphyrins play an important role in fabrication of electroluminescent [6] and photonic [7] devices used for photodynamic therapy [8], as well as for synthesis of materials with controllable magnetic properties [12]. Porphyrins can be incorporated into photochromic compounds used to store data [9] and to manufacture solar cells [10] and gas analyzers [11].

The porphyrin – fullerene pair is one of the optimal combinations for creating a bulk heterojunction. The C_{60} fullerene acts as a strong acceptor and is a widely available and inexpensive initial material for producing thin films by vacuum deposition [13]. Notably, thin films of pure porphyrin and porphyrin – fullerene nanocomposite are capable of supramolecular self-assembly and formation of molecular ensembles or aggregates [5, 14].

To date, the properties of porphyrins and various porphyrin-containing compounds have been studied mainly in solutions; however, it is solid structures and not solutions that have industrial applications [15]. One of the draw-

backs of organic structures, including fullerenes [16] and porphyrins [17], is that external factors can change their properties, mostly leading to degradation: photopolymerization occurs as a result of UV irradiation, exposure to oxygen or water vapor causes oxidation or photostimulated oxidation. The characteristics of the layers making up the structure are transformed in these cases [18].

There are practically no studies dealing with the effect of X-ray radiation (as an external factor) on the properties of composite porphyrin-fullerene films. This problem is rather poorly understood; for example, an increase in optical absorption below the edge of the Soret band was confirmed in [19] for CoMTPP films. On the other hand, the change in the properties of organic materials exposed to irradiation can lead not only to deterioration of the parameters that are important for practical applications, but also to modification and generating new useful characteristics [20].

A few more papers have reported on the effect of ionizing radiation on fullerenes; a number of studies confirmed the stability of their properties despite the effect of gamma irradiation [21]. The effect of various types of ionizing radiation on nanocomposite materials incorporating C_{60} fullerenes was considered in [22 – 24]. These studies found that adding fullerene improves the absolute stability of nanocomposites. Both an increase in crosslink density and an improvement in thermal stability of the nanocomposites incorporating fullerene were established in [23].

Ref. [24] is dedicated to applications of organic photovoltaic elements in outer space, where the elements are exposed to ionizing radiation. Changes in the characteristics depending on the irradiation dose for the P3HT:PCBM composite (polymer – fullerene) were attributed to the decay of the main chain and the reduction of π-conjugation in the P3HT polymer. The stability of the nanocomposites based on fullerenes with inorganic donors exposed to X-rays was demonstrated in [25].

In general, it can be argued that fullerene, due to its symmetry and the presence of a delocalized π-electron cloud, has enhanced stability against various types of ionizing radiation.

The study of degradation of the properties of porphyrin and fullerene – porphyrin films is an important task. This paper presents the comprehensive findings of an investigation of self-assembly processes and their effect on the structure of thin films of zinc tetraphenylporphyrin (ZnTPP) and nanocomposite films of zinc tetraphenylporphyrin with fullerene (ZnTPP – C_{60}). We have analyzed the changes in photoluminescence (degradation processes) in these films after exposure to X-ray radiation.

Sample preparation and methods of investigation

Sample preparation. A mixture consisting of both pure ZnTPP and a combination of ZnTPP и C_{60} in weight ratio of 1 : 1 was used to synthesize the films (both compounds were from Sigma-Aldrich, USA). BDS-10 grade boron-doped (111) silicon, freshly cleaved muscovite mica and potassium bromide (Kbr) were used as substrates.

While most studies use molecular beam epitaxy to grow organic films, we chose hot-wall epitaxy in quasi-equilibrium. This method allows to synthesize molecular crystals and obtain uniform nanocomposite films whose properties are highly reproducible under identical technological conditions. According to the data in [5, 14], film thickness ranges from 100 to 600 nm. The advantages of this method, in contrast to molecular beam epitaxy, are that it facilitates self-assembly and makes it possible for ordered structures of organic complexes to form.

The choice of temperature conditions was limited by the following factors. Firstly, the temperatures of the evaporator and the substrate were tailored to ensure minimal supersaturation of vapor in order to obtain self-assembling crystalline films. The condensation temperature of the films was chosen as close as possible to the evaporator temperature for this purpose. At the same time, the substrate temperature had to be maintained at a level below the evaporator temperature by 100 K in order to sustain the required growth rate and obtain pure films in a technical vacuum instead of an ultra-high one. Using a technical vacuum considerably simplifies the technology of growing the films and reduces the energy costs for synthesis.

Surface morphology studies. A JEOL JSM-6390 scanning electron microscope with the ultimate resolution of 3 nm was used for studying the self-assembly processes and the morphology of the surface and near-surface layers of the samples grown on Si (111) substrates.

Transfer processes and film composition in the selected local regions were investigated using an Oxford INCA Energy EDS microanalysis system for scanning electron microscopes with the ultimate sensitivity of 0.1 wt %. Samples grown on dielectric substrates, for example, on mica, cannot be studied by this method.

Film structure studies. The structure of the film samples was studied by X-ray diffractometry (XRD) for both silicon and dielectric substrates. The X8 PROTEUM diffractometer (Bruker, USA) was used.

Luminescence studies. Photoluminescence spectra were measured with an automated system consisting of a Horiba Jobin Yvon spectrometer and an FHR monochromator equipped with a Symphony II 1024*256 Cryogenic Open-Electrode CCD detector with a light yellow filter. Photoluminescence was excited by stabilized radiation of a semiconductor laser operating in continuous mode at a wavelength of 408 nm.

X-ray radiation. The samples were irradiated with different doses of X-rays from a tungsten-rhenium X-ray tube with the operating parameters of 40 kV and 90 mA. A tungsten-rhenium anode allowed to irradiate the samples with $K_{\alpha 1}$ and $K_{\beta 1}$ X-rays with the energies of 59.3 and 67.2 keV, respectively. The X-ray source was calibrated by changing the threshold voltage for MOS structures relative to that for the gamma radiation source.

The exposure doses were (in 10^5 R):

1.20; 2.65 and 4.51 for ZnTPP;

0.62; 1.45 and 2.69 for ZnTPP-C_{60}.

Irradiation and all measurements were carried out at room temperature (about 300 K).

Results and discussion

Scanning electron microscopy data. The surface morphology of the initial films is shown in Fig. 1. ZnTPP films exhibit a well-developed near-surface relief; their surface layer is an ordered, dense and clearly visible set of crystallites. Analysis of the film morphology in both secondary and elastically reflected electron fluxes revealed no impurity inclusions or inhomogeneities, with good reproducibility of the results.

It can be seen from Fig. 1, *b* that ZnTPP-C_{60} films have a more developed surface compared with ZnTPP and are a two-phase system with surface inclusions of the second phase in the form of nanorods. The second phase appears as the characteristic habit of porphyrin crystals and follows the laws of crystallography. The obtained surface morphology can be explained by the temperature conditions in which the films were synthesized and by the differ-

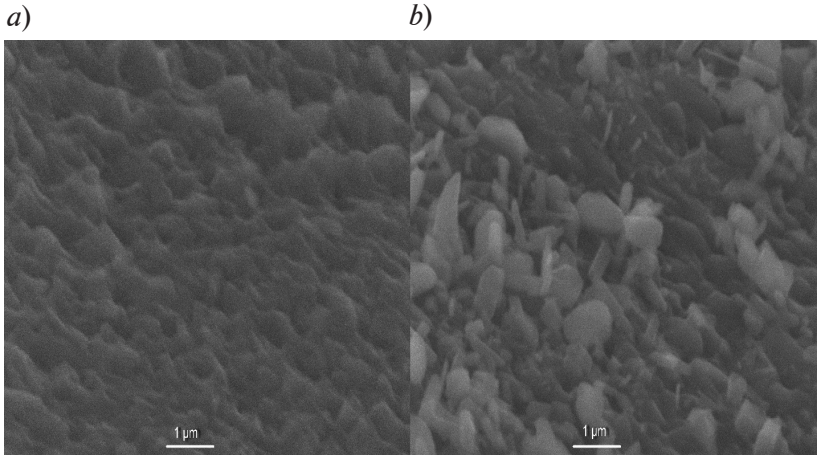

Fig. 1. Surface morphology of ZnTPP (*a*) and ZnTPP-C_{60} (*b*) films obtained by scanning electron microscopy

Table

Compositions determined for the studied compounds

Compound	Elemental composition, arb. units		
	Zn	C	N
ZnTPP	0,99	1,05	0,99
ZnTPP-C_{60}	1,24	0,95	1,52

Notes. 1. EDX was used. 2. The table lists the ratios of the obtained experimental values to the stoichiometric compositions of the thin-film samples studied.

ence in the evaporation temperatures of the C_{60} fullerene and ZnTPP. Since the evaporator and substrate heater is a rather massive graphite structure in the hot wall method, the films cooled down slowly after heating stopped. All the while, porphyrin, whose evaporation temperature is lower, kept evaporating from the remaining mixture. Crystallization in the form of nanorods was accompanied by weak interaction with the substrate and occurred with a small number of crystalline nuclei, which was facilitated by a persistently high temperature of the substrate.

Sample composition studies. The experimental results obtained by energy-dispersive X-ray microanalysis (EDX) confirm the above explanations. The data found were renormalized to exclude the contribution from the silicon substrate. A characteristic Si peak caused by this substrate is present in the spectral images with accelerating voltages of the primary electron beam of the order of 8 keV, since the penetrating power of such a beam is much greater than the thickness of the films in question. There was no point in using accelerating voltages of the primary electron beam below 8 keV, since the sensitivity of the method decreases sharply as a result. This method cannot be used to detect either hydrogen (since there are no electronic transitions in its atom) present in the composition of the organic materials under consideration or its weight contribution to the final result; thus, a systematic error is inevitably introduced into the measurements. For convenience, the experimental results obtained by EDX were normalized to the stoichiometric composition (see Table).

The normalization used allows to analyze the deviations of the experimental results from the values calculated from the initial mixture compositions; the results that fully coincide with the stoichiometric composition should yield a value of 1.00 in the table. Deviations towards depletion yield values less than unity, while enrichment is characterized by values greater than unity. It can be concluded from the data given in the table that the obtained ZnTPP film is practically stoichiometric, which means that nondestructive transfer of the composition of the initial mixture to the film occurs during the synthesis of the films.

An insignificant oxygen content (about 0.041 wt% for ZnTPP and 0.088 wt% for the composite) is not shown in the table and can be associated with free oxygen or oxygen in the water vapor adsorbed on the surface of the freshly grown film after it is removed from the vacuum chamber; this result does not necessarily indicate oxidation of the samples. The higher oxygen content in composite films may be due to a more developed surface of the sample.

Substantial deviations from the composition calculated from the initial mixture are observed for the ZnTPP-C_{60} nanocomposite film. The data point to carbon depletion of the obtained films with simultaneous zinc and nitrogen enrichment, i.e., enrichment in the porphyrin phase, which corresponds to SEM observations of porphyrin crystals in the second phase (see Fig. 1, *b*). According to calculations, the film contains approximately 38 % of fullerene instead of the 50 % weight in the initial composition. These results agree with the data for other types of composite films that we obtained earlier [14].

XRD analysis. More data on the structure of the films were obtained by analyzing

the samples grown on a silicon substrate (Fig. 2, *a*), on an oriented layered substrate of freshly cleaved of muscovite mica (Fig. 2, *b*) and on potassium bromide (Fig. 2, *c*). It was established in [26, 27] that a molecular crystal of ZnTPP can have a different structure, that is, exhibit polymorphism. According to the data in [28], the initial polycrystalline mixture consists of crystals with a triclinic system. However, the films obtained by the authors of that study under non-equilibrium conditions had an amorphous structure, and haloes were detectable in their XRD patterns only at scattering angles 2θ from 7° to 20°.

The processes of formation of polymorphic phases were studied in [29], where it was revealed that the activation energies of crystalline phases for different crystal systems can be classified in the following way by descending absolute values of crystal lattice energies:

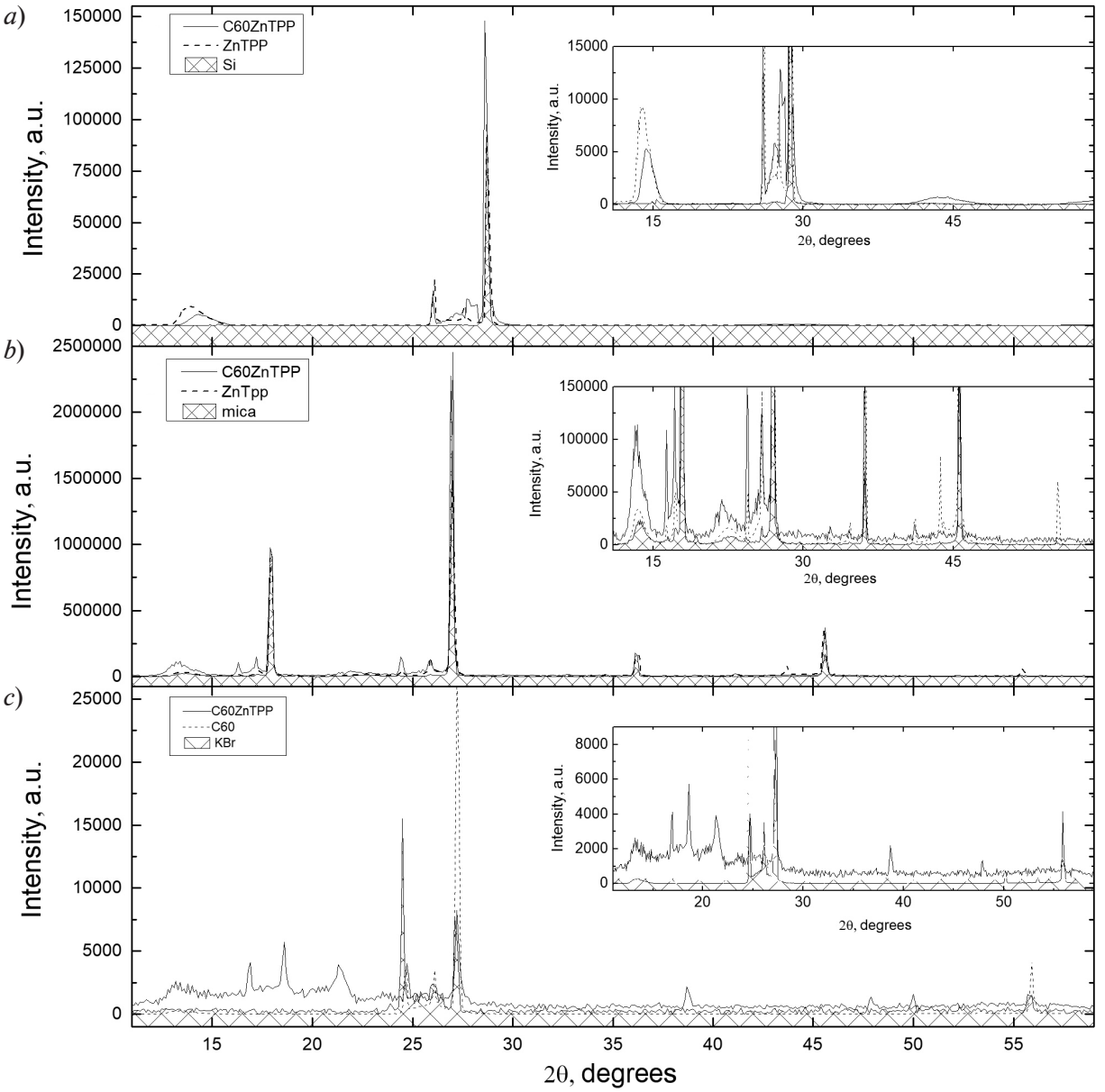

Fig. 2. XRD patterns of ZnTPP and ZnTPP-C_{60} films grown on different substrates: silicon (*a*), muscovite mica (*b*) and KBr (*c*).
The background and the peaks caused by X-ray diffraction from the substrates are shaded

$$P1 > I4/m > P2_1/n,$$

and the energies of the first two structural modifications are close and are significantly (by 15 kJ/mol) higher than the third one corresponding to the monoclinic system. Nucleation and growth of the $P2_1/n$ crystalline phase occur in the initial sample with the structure $I4/m$ in the temperature range of 443 – 493 K. Thus, we can expect structurally perfect ordered objects that correspond to a minimum energy to form in our samples.

Fig. 2, *a* shows the experimental XRD patterns of the film samples on Si (111) substrate. As the film's thickness is small, the main contribution is made by the peaks corresponding to the substrate; for silicon this is the peak with a scattering angle 2θ equal to 28.6°. A broad peak is observed in the XRD patterns of ZnTPP films in the range of 13 – 14°, which corresponds to the nanocrystalline component of the film, while a peak at 26.1° corresponds to ZnTPP crystals.

The position of the peaks is somewhat shifted for the composite, the prevailing type of crystal lattice cannot be determined reliably due to small intensities and a limited number of detected peaks; however, a large number of lines in the range of 2θ values from 25° to 27° likely corresponds to the $P1$ cell. The thin structure up to the intense silicon peak may be caused by the presence of various crystalline components in the ZnTPP-C_{60} film.

Analysis of the structure of dielectric oriented substrates of muscovite mica and potassium bromide was performed to refine the results obtained, and the degree of crystallinity of the films turned out to be higher in these cases. The number of spectral lines was much larger for the mica substrate than for the silicon and KBr substrates, and these lines largely overlapped the weaker peaks corresponding to the thin film; however, a set of lines from the nanocomposite can be detected after subtraction (the substrate peaks are shaded in Fig. 2): 10.9°; 13.2°; 16.3°; 17.2°, 21.9° and 24.4°. The set of lines corresponding to the crystalline structure of the composite is as follows for the KBr substrate: 13.2°; 16.8°; 17.2°; 21.3°; 38.7°; 47.8°.

The relative peak intensity is more difficult to estimate with the Debye – Scherrer method in the case of a thin film, since, in contrast to the powder, potential texturing of this film should be taken into account. However, a peak observed on dielectric substrates at 2θ values equal to 16 – 17° most likely excludes the presence of a phase with the $P2_1/n$ structure, as the intensity of the line is minimal for this phase in this region [29]. Apparently, the crystalline phase is deposited on the substrates in our experimental conditions but it may possibly belong to the $P1$ crystal system that is rather energetically unfavorable.

Spectral dependences of photoluminescence. It was established in the above-mentioned study [19] that X-ray irradiation changes the absorption spectrum below the HOMO-LUMO gap, so the photoluminescence method was chosen to investigate the changes in the electron spectrum.

Fig. 3, *a* shows the optical density spectra for ZnTPP both for the toluene solution and for the solid (film). The features of the spectra of ZnTPP solutions in Fig. 3 have already been well-studied [30, 31]. In addition to a strong band (the Soret band or the B band at a wavelength of 350 – 400 nm) due to allowed electronic transitions (the matrix element is not equal to zero), the so-called Q band, which is a set of bands in the visible region, is contained in the absorption spectra of porphyrins. In the case of D_{4h} molecular symmetry (metalloporphyrin), this region should consist of two bands. The Q band is quasi-forbidden, not on account of symmetry, but on account of cyclic conjugation [32], and is weak as a consequence. Two bands are present in the experimental absorption spectra in the Q region: their wavelengths are 550 and 590 nm. The first one is due to electron-vibrational (vibronic) replicas and is more intense because the oscillations act as a perturbing factor, removing the quasi-prohibition. A weak band at 590 nm in the absorption spectrum is caused by an electronic transition. The frequency difference in the absorption spectrum (590 and 550 nm in Fig. 3, *a*) should always be smaller than in the emission spectrum (600 and 650 nm in Fig. 3, *b*).

The positions of the absorption peaks in the spectrum remained the same for films, with the

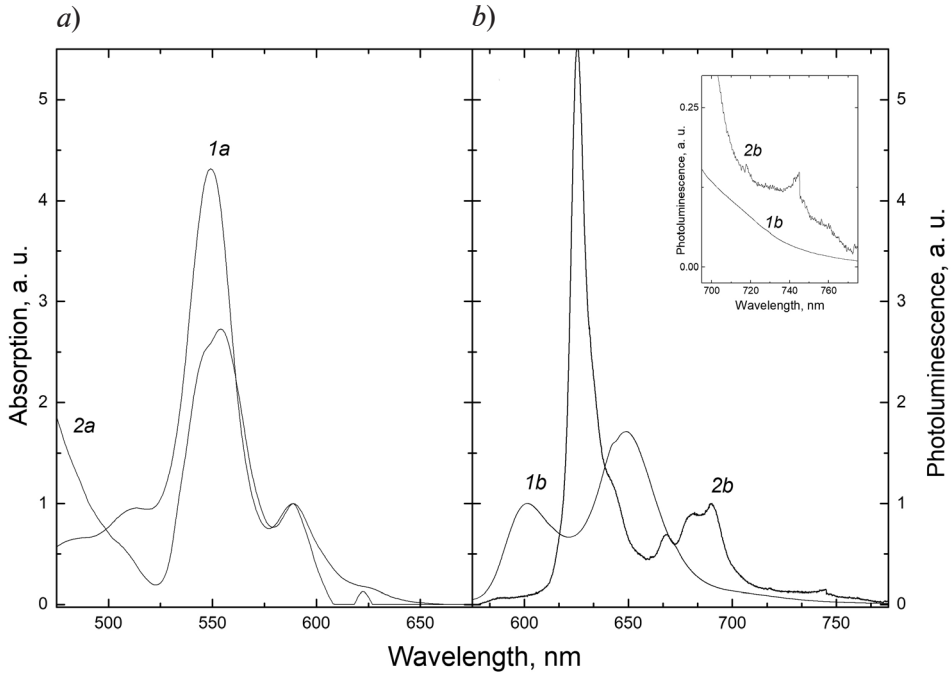

Fig. 3. Optical density (*a*) and photoluminescence (*b*) of ZnTPP solutions in toluene (*1a*, *1b*) and 300-nm-thick ZnTPP films on Si (111) substrate (*2a*, *2b*)

vibronic peak splitting into two components at 550 nm. Fig. 3, *b* shows the photoluminescence spectra of the films and the solution in toluene. Notably, there is a mirror symmetry in the position and intensity of the absorption and emission spectra for solutions, because the absorption and emission bands belong to the same electronic transition on which oscillations are superimposed; in other words, both spectra belong to the vibrational structure of one electronic transition [32].

However, the position and shape of the photoluminescence peaks for thin films do not correspond to those for the ZnTPP solution peaks.

Firstly, the photoluminescence spectrum of the films is shifted toward the long-wave region by approximately 30 nm. According to [33], the bathochromic shift is related to the stacking π-π interaction in the delocalized system of macrocyclic electrons during the formation of the ordered phase of porphyrin, mainly in the form of non-covalently bound $(ZnTPP)_2$ dimers.

Secondly, mirror symmetry breaks down for the intensities of the emission and absorption spectra in the solid-state phase, and the line associated with the electronic transition that was previously quasi-forbidden becomes the most intense in the emission spectrum.

Thirdly, the photoluminescence spectrum of films, in comparison with solutions, exhibits a new long-wave emission peak at 745 nm, apparently associated with phosphorescence. It was observed earlier that metalloporphyrin solutions possess phosphorescence, but only at low temperatures. Introducing a heavy or a paramagnetic atom into an organic molecule leads to a "mixing" of the wave functions of the singlet and triplet states, removing the rule forbidding intercombination, and, as a consequence, to an increase in the probability of singlet-triplet transitions. A molecule can relax from the excited state not only by conversion to the ground state, but also nonradiatively to a metastable triplet state [32]. In this case, spin-orbital interaction violates the rule forbidding intercombination. It can be concluded from the data obtained that the prohibition against intercombination can be violated due to formation of different kinds of structures, for example, porphyrin dimers.

The effect of X-ray radiation on the photoluminescence of samples. Photoluminescence

spectra of porphyrin and composite samples, recorded before and after irradiation with the respective doses, are shown in Fig. 4. It can be seen that the photoluminescence intensity is higher for the pure ZnTPP sample of (Fig. 4, *a*) than for the ZnTPP-C_{60} nanocomposite sample (Fig. 4, *b*). This is explained by fullerene's strong acceptor properties and the transfer of the photoexcited charge to the fullerene molecule in the ZnTPP-C_{60} nanocomposite [5]. A weaker change in the photoluminescence intensity than that obtained in [5] is in this case due to the formation of the second phase and fullerene depletion of the nanocomposite, compared with its stoichiometric composition. A decrease in photoemission intensity was observed after the first X-ray irradiation dose for all the samples studied, while the positions of the lines and their shapes remained in the spectrum. In order to clarify the behavior of photoluminescence intensity of the samples upon further irradiation, the obtained spectra were decomposed into the components of the Lorentz-type line and the dose dependences of the total relative intensity of the spectral fluorescence lines, caused by both electronic and vibronic transitions on energy scales, were plotted (Fig. 5), along with phosphorescence lines.

It can be seen from the graphs that the dose dependences of photoluminescence differ for the electronic and electron-vibrational components of the spectrum, both for pure ZnTPP films and for the composite. The intensity of the electron-vibrational component gradually decreases by 10 – 15 % as the

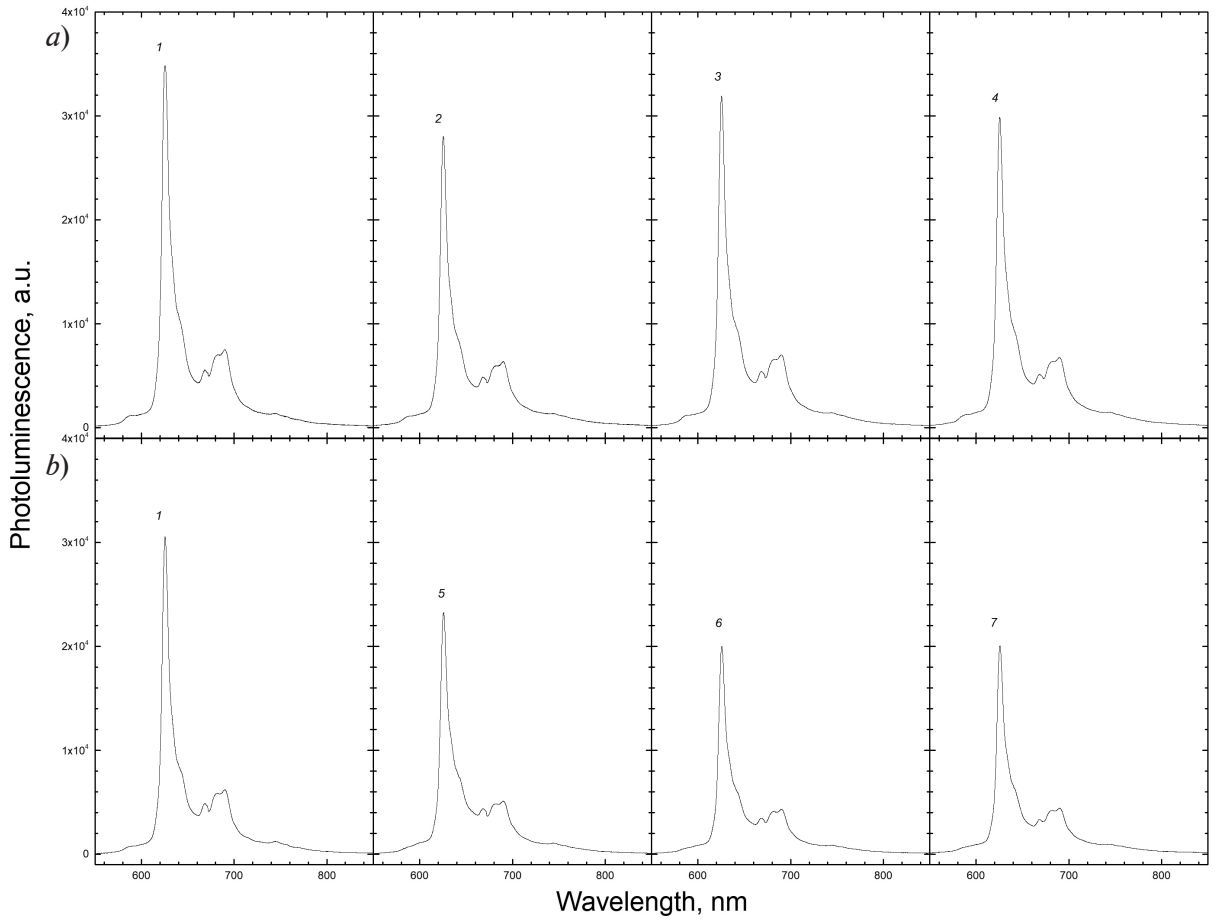

Fig. 4. Photoluminescence spectra of ZnTPP (*a*) and ZnTPP-C_{60} (*b*) films before irradiation (*1*) and after irradiation with different doses of X-rays (in 10^5 R): 1.20 (*2*); 2.65 (*3*); 4.51 (*4*); 0.62 (*5*); 1.45 (*6*); 2.69 (*7*)

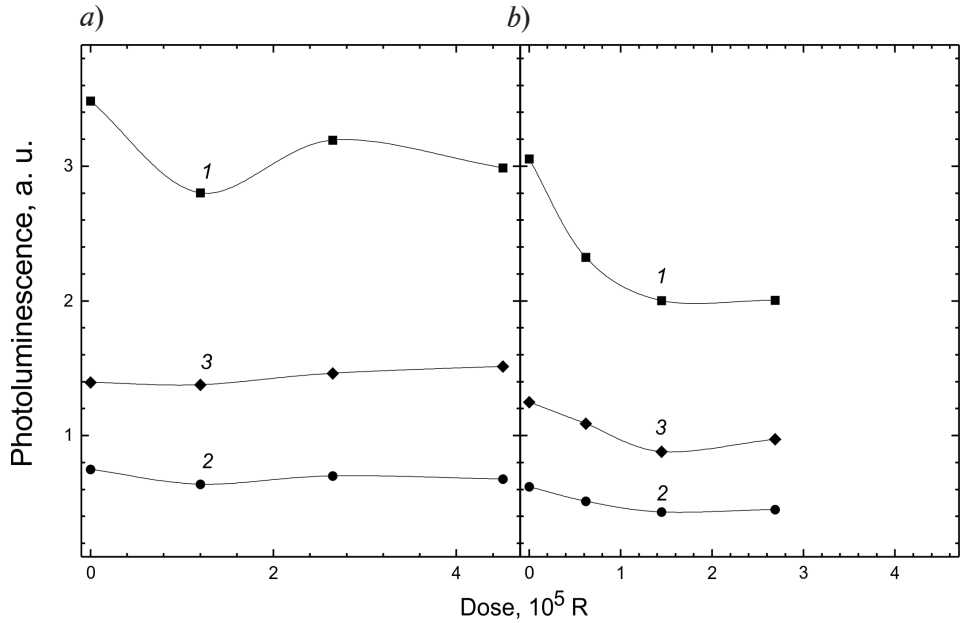

Fig. 5. Dependences of relative intensity of fluorescence (*1*, *2*) and phosphorescence (*3*) bands on the dose of X-rays for ZnTPP (*a*) and ZnTPP-C_{60} (*b*) samples.
The figure includes data for the peaks caused by electronic (*1*) and electron-vibrational (*2*) transitions

radiation dose increases. As for the electronic component of the fluorescence band, the dose dependence of its relative intensity is weaker for pure ZnTPP than for the composite material. While the intensity of the radiative electronic transition is practically restored after a 20 % drop for ZnTPP films, the decrease in intensity is more significant (by 5 0%) and monotonic for composite films.

The following assumptions have to be made to explain this form of the obtained dose dependences.

The effect of X-ray radiation for pure ZnTPP turns out to be weak in this range of doses and leads to an overall slight decrease in photoemission intensity associated with the growth of defects that contribute to nonradiative recombination. In this case, the relative contribution of phosphorescence slightly increases.

A stronger decrease in fluorescence intensity due to radiative electronic transition (up to 50 %) is observed for composite films, which is apparently because irradiation leads to an increased probability of luminescence quenching due to the energy transfer of carrier photoexcitation to fullerene.

Thus, it can be assumed that radiation defects developing in the composite compound under consideration (upon irradiation in the chosen dose range) lead to an increased probability of both intercombination transition and carrier photoexcitation transfer to the acceptor fullerene molecule. The effect should be more pronounced when the surface of the interface between the two phases increases.

Conclusion

This paper presents the results of investigations of thin films of zinc tetraphenylporphyrin (ZnTPP) and nanocomposite films of zinc tetraphenylporphyrin with fullerene (ZnTPP-C60) synthesized under quasi-equilibrium conditions.

We have studied the surface morphology of the samples by scanning electron microscopy and the structure of the films by X-ray diffractometry. Combining these methods, we were able to establish that a crystalline ZnTPP film formed on the silicon substrate and that a two-phase system was present in ZnTPP-C_{60} films at a phase ratio of 1.3 : 1.0 by weight.

Partial losses of the fullerene phase, compared with the calculated value, were discov-

ered in the ZnTPP-C_{60} composite films by energy-dispersive microanalysis.

The differences in the optical absorption and photoluminescence spectra in ZnTPP solutions and in the ZnTPP film synthesized indicate that an ordered phase is established. We have obtained data on the crystalline structure of the films with a *P*1-type lattice forming. Phosphorescence could be observed in crystalline ZnTPP films even at room temperature.

We have examined the changes in the photoluminescence spectra of thin films of ZnTPP and nanocomposite films of ZnTPP-C_{60} after X-ray irradiation with doses ranging from $1 \cdot 10^5$ до $3 \cdot 10^5$ R. We have found that films of pure ZnTPP with a coarse crystalline structure are sufficiently stable against these doses of X-ray radiation.

The dose dependences for composite ZnTPP-C_{60} films differ by the electronic and electron-vibrational contributions to photoluminescence intensity. A significant decrease (up to 50 %) in the intensity of the photoluminescence band due to electronic transfer is most likely linked to an increased probability of carrier photoexcitation transfer to fullerene molecules and, correspondingly, to an increased probability of photoluminescence quenching. In this case, the relative intensity of the electron-vibrational band in the photoluminescence spectrum of composite films only weakly depends on the irradiation dose, which can be explained by sufficiently high time constants of these processes.

REFERENCES

[1] **G. Dennle, M.C. Scharber, C.J. Brabec,** Polymer-fullerene bulk-heterojunction solar cells, Advanced Materials. 21 (13) (2009) 1323–1338.

[2] **P. Peumans, A. Yakimov, S.R. Forrest,** Small molecular weight organic thin-film photodetectors and solar cells, J. Appl. Phys. 93 (7) (2003) 3693–3723.

[3] **E.A. Katz,** Nanostructured materials for solar energy conversion, Ed. T. Soga, Elesevier, Amsterdam, 2006.

[4] **G. Mazzone, M.E. Alberto, B.C. de Simone, et al.,** Porphyrins and phthalocyanines in solar photovoltaic cells, J. Porphyrins Phthalocyanines. 14 (7) (2010) 759–792.

[5] **M.A. Elistratova, I.B. Zakharova, N.M. Romanov, et al.,** Photoluminescence spectra of thin films of ZnTPP-C_{60} and CuTPP-C_{60} molecular complexes, Semiconductors. 50 (9) (2016) 1191–1197.

[6] **Z. Guolun, J. Wu, Y. Wang, et al.,** Photo- and electroluminescent properties of 5,10,15,20-tetra-*p*-tolyl-21H,23H-porphine doped poly[2-methoxy-5-(2′-ethylhexyloxy)-1,4-phenylenevinylene] films, Thin Solid Films. 517 (11) (2009) 3340–3344.

[7] **D. Wrobel, A. Siejak, P. Siejak,** Photovoltaic and spectroscopic studies of selected halogenated porphyrins for their application in organic solar cells, Solar Energy Materials and Solar Cells. 94 (3) (2010) 492–500.

[8] **Y. Chen, G. Li, R.K. Pandey,** Synthesis of bacteriochlorins and their potential utility in photodynamic therapy (PDT), Current Organic Chemistry. 8 (12) (2004) 1105–1134.

[9] **J. Durantini, G.M. Marisa, S.M. Funes, et al.,** Synthesis and characterization of porphyrin electrochromic and photovoltaic electropolymers, Organic Electronics. 13 (4) (2012) 604–614.

[10] **K.D. Seo, M.J. Lee, H. MinSong, et al.,** Novel *D*-π-*A* system based on zinc porphyrin dyes for dye-sensitized solar cells: Synthesis, electrochemical, and photovoltaic properties, Dyes and Pigments. 94 (1) (2012) 143–149.

[11] **P. Muthukumar, J.S. Abraham,** Highly sensitive detection of HCl gas using a thin film of mesotetra(4-pyridyl)porphyrin coated glass slide by optochemical method, Sensors and Actuators. B. Chemical. 159 (1) (2011) 238–244.

[12] **M.A. Elistratova, I.B. Zakharova, O.E. Kvyatkovskii, et al.,** Electronic structure, optical and magnetic properties of tetraphenylporphyrins-fullerene molecular complexes, J. Phys., Conference Series. 690 (2016) 012012.

[13] **I.B. Zakharova, V.M. Ziminov, N.M. Romanov, et al.,** Optical and structural properties of fullerene films doped with cadmium telluride, Physics of the Solid State. 56 (5) (2014) 1064–1070.

[14] **N.M. Romanov, I.B. Zakharova,** The composition and the structure of thin films based on metalporphyrin complexes, St. Petersburg Polytechnical University Journal, Physics and Mathematics. (2) (2016) 1–7.

[15] **I. Fratoddi, C. Battocchio, R. D'Amato, et al.,** Diethynyl-Zn-porphyrin-based assemblies: optical and morphological studies of nanostructured thin films, Mat. Sci. Eng. 23 (6) (2003) 867–871.

[16] **R. Konenkamp, G. Priebe, B. Pietzak,** Carrier mobilities and influence of oxygen in C_{60} films, Phys. Rev. B. Condensed Matter and Materials

Physics. 60 (16) (1999) 11804–11808.

[17] **E.V. Antina, E.V. Balantseva, M.B. Berezin,** Oxidative degradation of porphyrins and metalloporphyrins under polythermal conditions, Russian Journal of General Chemistry. 81 (6) (2011) 1222–1230.

[18] **H. Kim, W. Kim, Y. Mackeyev, et al.,** Selective oxidative degradation of organic pollutants by singlet oxygen-mediated photosensitization: tin porphyrin versus C_{60} aminofullerene systems, Environ Sci. Technol. 46 (17) (2012) 9606–9613.

[19] **M.M. El-Nahass, A.H. Ammar, A.A. Atta, et al.,** Influence of X-ray irradiation on the optical properties of CoMTPP thin films, Optics Commun. 284 (9) (2011) 2259–2263.

[20] **D. Manas, M. Manas, M. Stanek, et al.,** Micromechanical properties of surface layer of HDPE modified by beta irradiation, Intern. J. Mech. 8 (2014) 150–157.

[21] **V.A. Basiuk, G. Albarrбn, E.V. Basiuk, J.-M. Saniger,** Stability of interstellar fullerenes under high-dose γ-irradiation: new data, Advances in Space Research. 36 (2) (2005) 173–177.

[22] **M.A. Elistratova, I.B. Zakharova, N.M. Romanov,** X-ray radiation influence on photoluminescence spectra of composite thin films based on C_{60}<CdTe>, J. Phys., Conf. Ser. 586 (2015) 012002.

[23] **F. Cataldoa, O. Ursinib, G. Angelinib,** Radiation-cured polyisoprene/C_{60} fullerene nanocomposite, Part 2, Synthesis in decalin, Rad. Phys. Chem. 77 (6) (2008) 742–750.

[24] **A.M. Todd, T. Zhua, F. Zhang, et al.,** Performance degradation of P3HT:PCBM polymer/ fullerene photovoltaic cells under gamma irradiation, ECS Trans. 25 (11) (2009) 103–111.

[25] **N.M. Romanov, I.B. Zakharova, E. Lähderanta,** Diagnostics of thin films of fullerene / cadmium telluride and their stability under X-ray radiation by IR spectroscopy // Optical Journal. 84 (12) (2017) 50–55.

[26] **G.L. Perlovich, O.A. Golubchikov, M.E. Klueva,** Thermodynamics of porphyrin sublimation, J. Porphyrins Phthalocyanines. 4 (8) (2000) 699–706.

[27] **M.P. Byrn, C.J. Curtis, Y. Hsiou, et al.,** Porphyrin sponges: conservative of host structure in over 200 porphyrin-based lattice clathrates, J. Am. Chem. Soc. 115 (21) (1993) 9480–9497.

[28] **H.M. Zeyada, M.M. Makhlouf, M.A. Ali,** Structural, optical and dispersion properties of 5,10,15,20-tetraphenyl-21H,23H-porphyrin zinc thin films, J. Appl. Phys. 55 (2) (2016) 022601–022608.

[29] **G.L. Perlovich, W. Zielenkiewicz, Z. Kaszkur, et al.,** Thermophysical and structural properties of crystalline solvates of tetraphenylporphyrin and their zinc, copper and cadmium metallo-complexes, Thermochimica Acta. 311 (1-2) (1998) 163–171.

[30] **R.T. Kuznetsova, E.G. Ermolina, R.M. Gadirov, et al.,** Luminescence of metal complexes of chelate substituted tetraphenylporphyrin, High Energy Chemistry. 44 (2) (2010) 134–138.

[31] **M. Gouterman,** Optical spectra and electronic structure of porphyrins and related rings, The Porphyrins, Vol. 3, Ed. D. Dolphin, Academic Press, New York (1978) 161–165.

[32] **G.P. Gurinovich, A.N. Sevchenko, K.N. Solov'ev,** The spectroscopy of the porphyrins, Soviet Physics Uspekhi. 6 (1) (1963) 67–105.

[33] **X.-L. Zhang, J.-W. Jiang, Y.-T. Liu, et al.,** Identifying the assembly configuration and fluorescence spectra of nanoscale zinc-tetraphenylporphyrin aggregates with scanning tunneling microscopy, Sci. Rep. 6 (2016) 227561–227567.

Received 06.02.2018, accepted 03.03.2018.

THE AUTHORS

ROMANOV Nikolay M.
Peter the Great St. Petersburg Polytechnic University
29 Politechnicheskaya St., St. Petersburg, 195251, Russian Federation
nikromanov.90@gmail.com

ZAKHAROVA Irina B.
Peter the Great St. Petersburg Polytechnic University
29 Politechnicheskaya St., St. Petersburg, 195251, Russian Federation
zakharova@rphf.spbstu.ru

ELISTRATOVA Marina A.
Ioffe Institute of RAS
26 Politechnicheskaya St., St. Petersburg, 195251, Russian Federation
marina.elistratova@mail.ioffe.ru

LÄHDERANTA Erkki
Lappeenranta University of Technology
Skinnarilankatu 34, 53850 Lappeenranta, Finland
Erkki.Lahderanta@lut.fi